PAPER

Performance Evaluation of Variable Bandwidth Channel Allocation Scheme in Multiple Subcarrier Multiple Access

Nitish RAJORIA[†a)], Hiromu KAMEI[†], *Nonmembers*, Jin MITSUGI[††], Yuusuke KAWAKITA[†††], *and* Haruhisa ICHIKAWA[†††], *Members*

SUMMARY Multiple Subcarrier Multiple Access (MSMA) enables concurrent sensor data streamings from multiple wireless and batteryless sensors using the principle of subcarrier backscatter used extensively in passive RFID. Since the interference cancellation performance of MSMA depends on the Signal to Interference plus Noise Ratio of each subcarrier, the choice of channel allocation scheme is essential. Since the channel allocation is a combinatorial problem, obtaining the true optimal allocation requires a vast amount of examinations which is impracticable in a system where we have tens of sensor RF tags. It is particularly true when we have variable distance and variable bandwidth sensor RF tags. This paper proposes a channel allocation scheme in the variable distance and variable bandwidth MSMA system based on a newly introduced performance index, total contamination power, to prioritize indecision cases. The performance of the proposal is evaluated with existing methods in terms of average communication capacity and system fairness using MATLAB Monte Carlo simulation to reveal its advantage. The accuracy of the simulation is also verified with the result obtained from the brute force method.

key words: *passive communications, wireless sensing, multiple access, subcarrier allocation*

1. Introduction

RFID is a wireless technology that enables identification and monitoring of physical objects by affixing passively powered RF tags to physical objects [1], [2]. Recently, the integration of sensor into passive RFID tags becomes popular. A RFID tag integrated with sensor, usually referred to as a sensor RF tag, can acquire its surrounding condition such as temperature, humidity, pressure, acceleration. Usually, the data from sensor RF tag is captured by a reader in a time division manner whereas some applications require collecting sensor data from multiple sensors concurrently to take the correlation of sensor data streams.

An example use of concurrent sensor data streaming is the integrity testing of civil structures (machinery, airplane, artificial satellite, building etc) [3], [4]. Conventionally in these testings, accelerometers or strain sensors are wired and attached to the target structure and all the sensors are powered and monitored through the wires. Routing such wires takes time and labors, and thus, frequent integrity testings become inhibitive. This is why many research target batteryless and wireless structural health testing [5]–[8]. These tests often demand a concurrent acquisition from many, say up to fifty, sensor RF tags.

We have been proposing Multiple Subcarrier Multiple Access (MSMA) [9] to enable concurrent sensor data streamings from multiple batteryless and wireless sensor RF tags. The principal idea of MSMA is the simultaneous usage of multiple subcarrier backscatters. The harmonics inevitably produced by a subcarrier backscatter can be cancelled by a set of signal processing in a software defined receiver. Since the performance of the interference rejection depends on the signal-to-interference-plus-noise ratio (SINR) of subcarriers before the rejection, it is essential to optimally allocate subcarriers to sensor RF tags in the reading zone [10]. The detail of MSMA principle is explained in Appendix A for the completeness of this paper.

Figure 1 overviews MSMA workflow. A reader firstly inventories sensor RF tags in its reading zone. Based on the collected tag IDs, the reader assigns subcarrier frequencies to each sensor RF tag. After the allocation, all the sensor RF tags stream sensor data on the allocated subcarrier without time synchronization. Naturally, MSMA is advantageous where a long duration concurrent data streaming, such as integrity testing of civil structure, is demanded.

Authors previously reported on the channel allocation problem in MSMA [11], where all the sensor RF tags demand an equal subcarrier bandwidth. Four allocation schemes were examined to reveal that allocating low subcarriers (low denotes the subcarrier is closed to the powering carrier frequency) to the geographically remote sensor RF tags and high subcarriers (subcarriers whose frequency is relatively far from the carrier frequency) to the geographically close sensor RF tags is, in general, advantageous in terms of the total communication capacity and fairness [12].

Subcarrier optimization problem is also investigated in OFDMA field. In [13], [14], several subcarrier allocation schemes based on game theory are proposed for achieving channel gain and power allocation. Such allocation schemes are not applicable in sensor RF tags, because even basic signal processing such as inverse FFT and channel filtering are prohibitive in batteryless backscatter communication system. Dynamic programming such as knapsack problem

Manuscript received January 13, 2017.
Manuscript revised June 4, 2017.
Manuscript publicized August 3, 2017.

[†]The authors are with Graduate Student, Graduate School of Media and Governance, Keio University, Fujisawa-shi, 252-0882 Japan.
[††]The auhor is with Faculty of Environment and Informations Studies, Keio University, Fujisawa-shi, 252-0882 Japan.
[†††]The authors are with Graduate School of Informatics and Engineering, University of Electro-Communications, Chofu-shi, 182-8585 Japan.
a) E-mail: nitish@keio.jp

DOI: 10.1587/transcom.2017EBP3016

could be applied to the channel allocation problem. But the existence of infinite harmonics in the multiple subcarrier system complicates the problem particularly when we allow variable subcarrier bandwidth.

In this paper, we extend our study to the channel allocation for variable subcarrier bandwidth MSMA. An exemplary variable bandwidth MSMA is where some sensor RF tags send only one axis acceleration measurement while others send three axes measurements. We show there are indecision cases where the two priorities on bandwidth and distance contradict. We introduce single performance index, total contamination power, to prioritize such indecision cases. The performance of the proposed scheme is evaluated with existing schemes in terms of the average communication capacity and system fairness using MATLAB.

The rest of paper is organized as follows: In Sect. 2, the problem of variable bandwidth subcarrier allocation in MSMA and the goal of the study are defined. In Sect. 3 we explain four candidate allocation schemes deduced from the previous studies. In Sect. 4, the simulation setup and analysis of results are introduced, and finally, Sect. 5 concludes the paper.

2. Problem Statement and Evaluation Model

Let there be N sensor RF tags, each indexed as T_i ($i = 1 \dots N$), located at distance r_i from the reader. i-th sensor RF tag requires bandwidth b_i Hz at the subcarrier frequency f_i Hz. Let us assume that the available bandwidth, B Hz, is equal to the sum of the bandwidth $B = \sum_{i=1}^{N} b_i$. To denote the variable bandwidth, the total bandwidth B is sub-divided into unit channels. This way, an arbitrary bandwidth can be represented as an aggregation of unit channels called subcarrier. The received signal power (S_i) of i-th subcarrier at the reader depends on the distance r_i of sensor RF tag from the reader. Since we assume the free space loss as propagation model, the received signal power is proportional to $1/r_i^4$ of the transmitted power. However, the other propagation models such as extended HATA SRD [15] can be applied with appropriate simulation parameters.

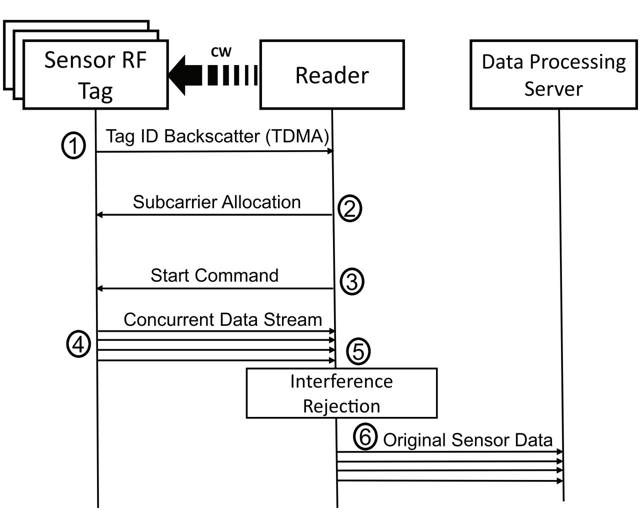

Fig. 1 Basic work flow of multiple subcarrier multiple access.

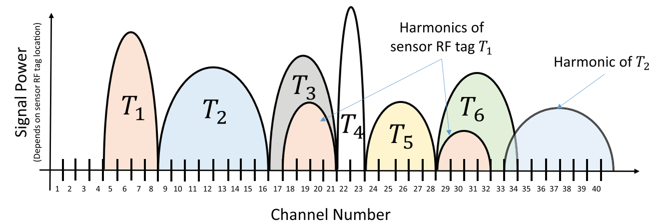

Fig. 2 Harmonics interfere to other subcarriers, when subcarrier bandwidth is variable.

In MSMA, a subcarrier inevitably produces harmonics on odd multiples of primal subcarrier frequency. A subcarrier ($f_i \pm b_i/2$) generates harmonics to other subcarrier bands as in Eq. (1) with signal power (S_i/n^2) and thereby creates harmonic noise to the sensor RF tags operating at those frequencies.

$$n f_i \pm \frac{b_i}{2}, n = 3, 5, 7, \cdots \tag{1}$$

The harmonic noise h_{ij} created on f_j from other subcarriers f_i can be calculated as shown in Eq. (2). Therefore, the total interference, H_j on a subcarrier f_j is obtained by adding the all harmonic noise on it as in Eq. (3). It is clear that only a limited group of subcarrier frequencies f_i ($i \leq \frac{j}{3}$) incur harmonics on f_j.

$$h_{ij} = \begin{cases} \frac{S_i}{n^2} & if(\frac{j}{i} = n = 3, 5, 7 \cdots) \\ 0 & else \end{cases} \tag{2}$$

$$H_j = \sum_{i=1}^{\lfloor j/3 \rfloor} h_{ij} \tag{3}$$

The communication capacity E_i of i^{th} sensor RF tag is quantified with Shannon formula (Eq. (4)) where the SINR for the i^{th} sensor RF tag is represented as $SINR_i$. The total system capacity can be obtained by simply adding individual communication capacity for all the sensor RF tags as in Eq. (5) where n_T denotes the constant thermal noise coefficient.

$$E_i = \sum_{i=1}^{N} b_i \log_2(1 + SINR_i) \tag{4}$$

$$E = \sum_{i=1}^{N} E_i = \sum_{i=1}^{N} b_i \log_2(1 + \frac{S_i}{H_i + n_T b_i}) \tag{5}$$

The problem is to divide B Hz into N subcarrier bands ($f_i \pm b_i/2$) and allocate to N sensor RF tags such that the total communication capacity E is maximized. An example of channel allocation is shown in Fig. 2. It should be noted that some of the interference may spread over more than one unit channel as shown in Fig. 2.

3. Channel Allocation Scheme

In the previous paper [11], we reveal that the allocating low

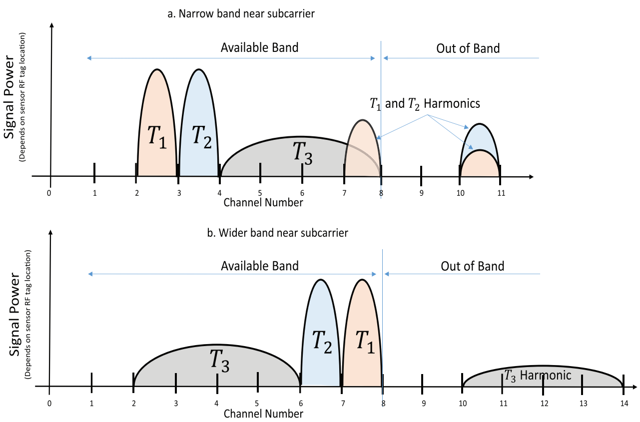

Fig. 3 An example to compare NB and WB allocation schemes.

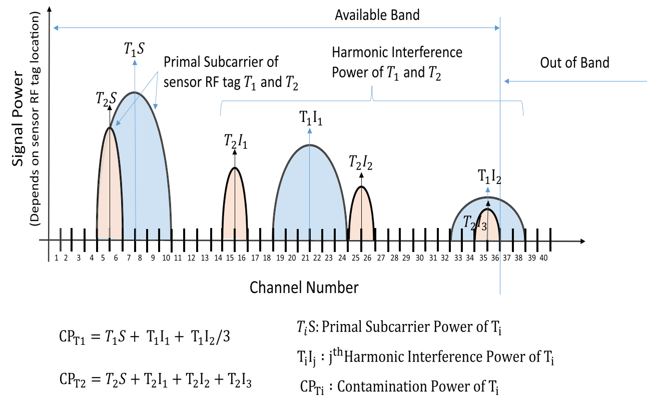

Fig. 4 Comparison of contamination power for sensor RF tag T_1 and T_2 located at different distance and required different badwdith.

frequencies to remote sensor RF tags principle works for a constant subcarrier bandwidth MSMA system. We denote this as FT (Far Tags to low frequency) scheme. A straightforward extension of the principle which prioritizes less interfering subcarriers to low frequencies, to the variable bandwidth MSMA is to allocate low frequencies to wide bandwidth subcarriers. We denote this as WB (Wide Bandwidth to low frequency) scheme. We also examine the reverse priority, which is to allocate low frequencies to narrow bandwidth subcarriers. We referred this to as NB (Narrow Band to low frequency) scheme expecting NB is inferior to WB.

Figure 3 shows a comparison of NB and WB schemes when three sensor RF tags are located at the same distance. It is shown that the harmonics produced by narrow bandwidth sensor RF tag (T_1) fall in the available bandwidth when narrow bandwidth sensor RF tag is prioritized (allocated first). On the other hand, when the wide bandwidth sensor RF tag (T_3) is prioritized there is no harmonics in the available bandwidth. The reason of NB's inferiority to WB is the wide spread of harmonics in the available bandwidth.

This comparison of NB and WB provides an insight of general performance index. Apparently, the indecision case is when we try to prioritize either a wide bandwidth sensor RF tag close to the reader or a narrow bandwidth sensor RF tags located remote from the reader. As a simple index to prioritize such indecision cases, we invent an index referred to as contamination power (CP). CP is the summation of power of both principal subcarrier and harmonics in the available bandwidth as shown in Fig. 4, where we calculate the contamination power for sensor RF tags T_1 and T_2 when subcarriers allocated to first T_1 or T_2. Later, the scheme choose the sensor RF tag which produces the less contamination power in the available band.

We refer this as to CP scheme. CP scheme basically tries to reduce the total power into the available bandwidth. Prioritizing the small contamination power sensor RF tags to low frequencies, regardless of distance and the bandwidth is expected to minimize the interference and consequently results in a good communication capacity.

The pseudo codes of the four schemes are listed in Algorithms 1–4.

Algorithm 1 FT: Far Tag Near Subcarrier

T is a list of sensor RF tags, arranged in decreasing order based on their distance.
C is the total number of channels. Initialize $i = 1$ and $j = 0$;
while $j! = \lceil C/3 \rceil$ **do**
  Pick the sensor RF tag T_i from the list, say, requires c unit channels.
  Allocate c unit channels from j to $j + c$ to T_i, delete T_i from the list.
  $i \rightarrow i + 1$; $j \rightarrow j + c$;
end while
Arrange the list T in reverse order.
Pick a sensor RF tag from the list, allocate its require unit channels and continue this step.

Algorithm 2 WB: Wide Bandwidth to low subcarriers

T is a list of sensor RF tags, arranged in decreasing order based on their required channel badnwidth.
C is the total number of channels. Initialize $i = 1$ and $j = 0$;
while $j! = \lceil C/3 \rceil$ **do**
  Pick the sensor RF tag T_i from the list, say, requires c unit channels.
  Allocate c unit channels from j to $j + c$ to T_i, delete T_i from the list.
  $i \rightarrow i + 1$; $j \rightarrow j + c$;
end while
Arrange the list T in increasing order based on sensor RF tag location.
Pick a sensor RF tag from the list, allocate its require unit channels and continue this step.

Algorithm 3 NB: Narrow Bandwidth to low subcarriers

T is a list of sensor RF tags, arranged in increasing order based on their required channel badnwidth.
C is the total number of channels. Initialize $i = 1$ and $j = 0$;
while $j! = \lceil C/3 \rceil$ **do**
  Pick the sensor RF tag T_i from the list, say, requires c unit channels.
  Allocate c unit channels from j to $j + c$ to T_i, delete T_i from the list.
  $i \rightarrow i + 1$; $j \rightarrow j + c$;
end while
Arrange the list T in increasing order based on sensor RF tag location.
Pick a sensor RF tag from the list, allocate its require unit channels and continue this step.

Algorithm 4 CP: low Contamination Power to low subcarriers

T is a list of all sensor RF tags.
C is the total number of unit channels.
U is the used channels.
Initialize $U = 0$ and $i = 1$.
while $U <= \lceil C/3 \rceil$ **do**
  for $< j = 1 : N + 1 - i >$ **do**
    Calculate contamination power for the sensor RF tag T_j.
  end for
  Find the sensor RF tag t has minimum contamination power, calculated in last step.
  Assign the sensor RF tag t to its require channels, say, c. Delete the sensor RF tag t from the list T.
  $i \rightarrow i + 1$; $U \rightarrow U + c$
end while
Arrange the list T in increasing order based on sensor RF tag location.
Pick a sensor RF tag from the list, allocate its require unit channels and continue this step.

4. Evaluation

A Monte Carlo simulator is developed with MATLAB to evaluate the proposal and the counter schemes. In one round of Monte Carlo simulation, N sensor RF tags are randomly distributed in a circular region of radius 10 meter where the reader is always located at the center. The minimum distance between the reader and the sensor RF tag is set to be 1 meter. Table 1 shows the details of simulation parameters.

The four schemes, FT, WB, NB and CP, are applied in each round, if applicable, and the total communication capacity divided by the number of sensor RF tags and the channel allocation are recorded. After the completion of predefined number of simulation rounds, the average communication capacity of the four schemes are derived. The pseudo code of X times Monte Carlo simulation is shown in Algorithm 5.

Algorithm 5 Simulation Method

for $< i = 1 : X >$ (X = 100, number of simulation runs) **do**
  Random and uniform distribution of N sensor RF tags in the circular region
  for $< j = 1 : Y >$ (Y is different allocation schemes) **do**
    Allocate subcarrier channels according to scheme
    Evaluate signal power and harmonic noise power on each sensor
    Evaluate signal to noise ratio (SINR), average communication capacity, fairness index
  end for
end for
Generate average performance parameters for each allocation scheme

To denote a set of variable bandwidth, we introduce "Class" which denotes the number of required unit channels and "Scenario" which denotes the distribution of sensor RF tags in each Class. We use four Classes and two Scenarios as in Table 2 such that each scenario provides the same available bandwidth. A general formula to calculate available bandwidth in particular Scenario is, C1 sensor RF tags $\times$ 1 + C2 sensor RF tags $\times$ 2 + C3 sensor RF tags $\times$ 3 + C4 sensor RF tags $\times$ 4. (For example, if there is eight sensor RF tags in Scenario 1, total available channels = $2 \times 1 + 2 \times 2 + 2 \times 3 + 2 \times 4 = 20$ channels. To provide the same bandwidth in Scenario 2, ten sensor RF tag are considered, total available channels = $4 \times 1 + 3 \times 2 + 2 \times 3 + 1 \times 4 = 20$ channels.)

Table 1 Simulation setup parameter.

Simulator	Matlab
Unit channel bandwidth	1 KHz
Network layout	Single-cell with omni-direction antenna
Total # of Subcarrier	Equal to # of sensor RF tag
Reader antenna gain	0 dBi
Reader transmitting power	1W
Sensor RF tag position	Stationary

Table 2 Distribuition of sensor RF tags in four classes.

Class Number	Rq. # of channels	Scenario-1	Scenario-2
C1	1	25%	40%
C2	2	25%	30%
C3	3	25%	20%
C4	4	25%	10%

To show the advantage of CP scheme, we evaluate the following three different simulation cases.

1. The first case is where all the sensor RF tags demand an equal bandwidth. In this case, only CP and FT are used. CP shall provide the equivalent allocation and performance to FT.
2. The second case is where all the sensor RF tags are located at the same distance and demand different bandwidth subjected to Scenario 1. In this case CP scheme shall provide the same allocation and performance to WB.
3. The third case is where sensor RF tags demand variable bandwidth based on a scenario and their distances from the reader are randomly chosen. We also show the superiority of CP regardless of the choice of scenario.

Finally, the accuracy of simulation is verified by comparing results with the brute force method for eight sensor RF tags. For more than eight sensor RF tags, the brute force method computation is intensive and infeasible even with a high-performance workstation (HP Workstation Z230 - Xeon E3-1245V3 3.4 GHz) because of significant number of permutation combinations.

4.1 Case-1: Sensor RF Tags Require Equal Bandwidth Subcarrier Located at Varying Distance

Figure 5 shows the comparison of average communication capacity with FT and CP schemes, when all sensor RF tags require equal bandwidth. All sensor RF tags are considered to be in Class C1. It can be seen that both CP and FT have similar performance. The average communication capacity of both schemes decrease as the number of sensor RF tag

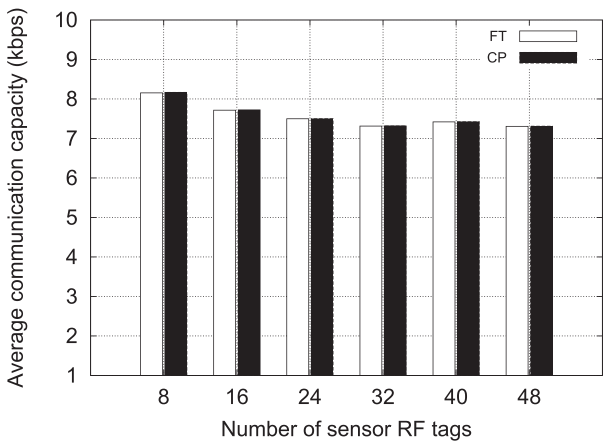

Fig. 5 Comparison of average communication capacity for FT and CP schemes when all sensor RF tags require unit bandwidth channel in Scenario-1.

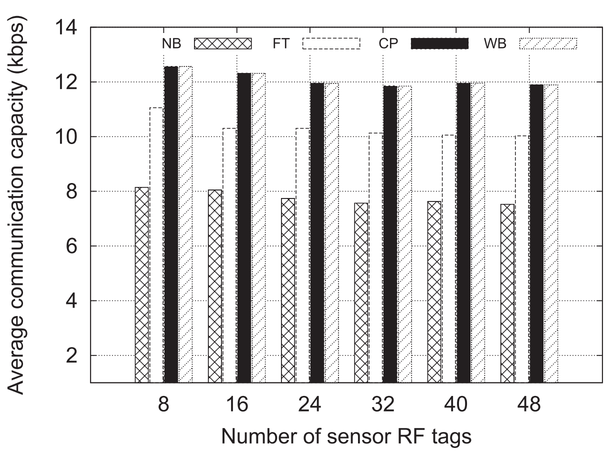

Fig. 6 Comparison of average communication capacity when all sensor RF tags are located at equal distance (6 meter) in Scenario-1.

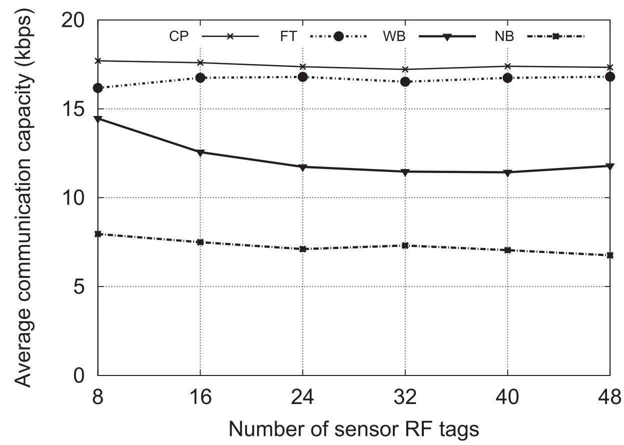

Fig. 7 Comparison of average communication capacity for different allocation scheme in Scenario 1.

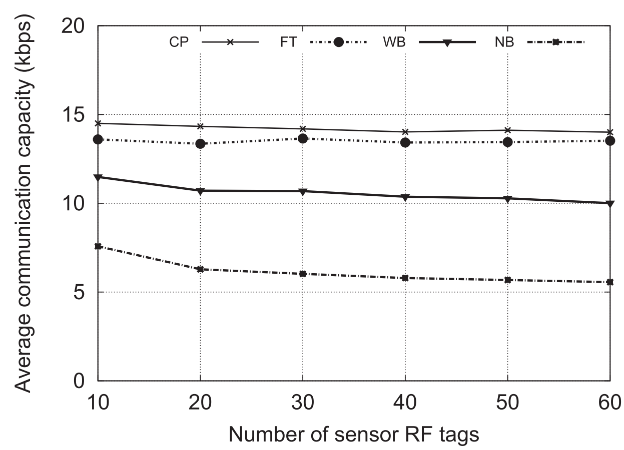

Fig. 8 Comparison of average communication capacity for different allocation scheme in Scenario 2.

increases. This is because the number of harmonics in the available bandwidth increases as the number of sensor RF tags increases.

4.2 Case-2: Sensor RF Tags Located at Same Distance Require Varying Bandwidth Subcarrier

All four allocation schemes are evaluated for this case and the results are shown in Fig. 6. The fixed distance of the sensor RF tags is chosen to be 6 m. It can be seen that CP scheme performs best and equivalently to WB. FT does not perform well because FT cannot prioritize the bandwidth. NB shows the worst performance as predicted.

4.3 Case-3: Sensor RF Tags Located at Varying Distance Require Varying Bandwidth Subcarrier

The average communication capacity with the four schemes subjected to Scenarios 1 is shown in Fig. 7. It is shown CP outperforms other schemes. FT performs closely to CP while WB contributes little. The difference of FT and WB performance can be explained such that the difference of distance spans from 1m to 10m which results in 10000 times difference with the free space loss assumption while the difference of bandwidth is four at most. NB performs worst in this case too. We confirm the robustness of CP in Scenario 2 as shown in Fig. 8.

For this particular case, we evaluate the system fairness for Scenario 1. Figure 9 shows the fairness of the four schemes. FT and CP show equivalent and best performance. The achieved fairness 0.8, which is not necessarily good, stems from the wide variation in sensor RF tags location (far and close to the reader) compare to their require bandwidth.

4.4 Examination CP Scheme with Brute Force Method

For verification, CP scheme is compared with the brute force method with eight sensor RF tags under Scenario 1. As in the other simulation cases, we examine 100 times Monte Carlo simulations. In the brute force method, we examine all the permutational combinations and extract the allocation which gives the best average communication capacity. The total number of combinations we examine is, therefore,

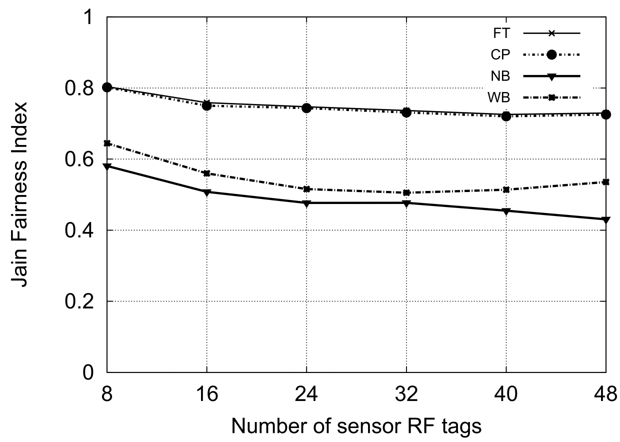

Fig. 9 Comparison of fairness index for different allocation scheme.

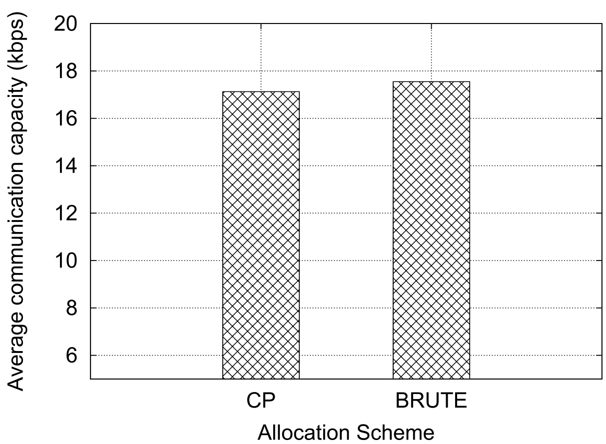

Fig. 10 Comparison of average communication capacity of CP scheme and brute force for eight sensor RF tags.

Table 3 An example to compare subcarrier allocation pattern for CP scheme and brute method.

Sensor RF tag	T_1	T_2	T_3	T_4	T_5	T_6	T_7	T_8	-
Rq. channels	1	1	2	2	3	3	4	4	-
Located at	2.6	9.5	4.7	5.0	8.7	6.3	5.1	3.1	-
Subcarrier #	1	2	3	4	5	6	7	8	capacity
CP	T_5	T_2	T_6	T_1	T_8	T_3	T_4	T_7	16.01
Brute	T_5	T_2	T_7	T_1	T_6	T_3	T_8	T_4	16.45

40320 = 8! for eight sensor RF tags.

Figure 10 shows the average communication capacity of CP scheme and the brute force method. It is shown CP performs equivalently to the brute force method but not exactly. To understand the difference, we compare the allocation outcomes from one round of simulation in Table 3 and also the allocation pattern shows pictorially in Fig. 12. CP and the brute force method both prioritize sensor RF tag T_5 over sensor RF tag T_2 where the two sensor RF tags are in indecision combination — sensor RF tag T_5 demands a wider bandwidth whereas it is relatively near the reader compared to sensor RF tag T_2. Both schemes choose differently for the third subcarrier. This is also an indecision case of sensor RF tags T_6 and T_7. CP chooses T_6 instead of

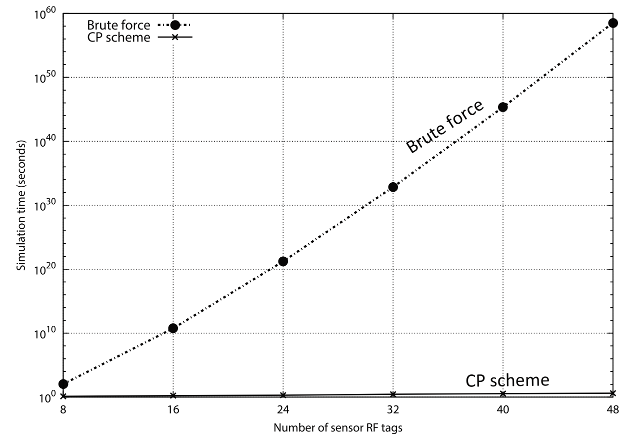

Fig. 11 Comparison of simulation execution time for CP scheme and brute force calculated theoretically.

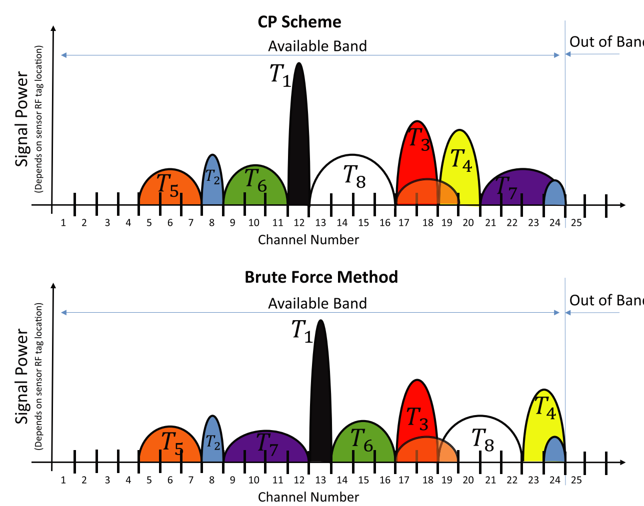

Fig. 12 The pictorial representation of allocation pattern for CP scheme and brute method.

T_7 because either choice does not generate harmonic in the available bandwidth. In terms of the contamination power, therefore, the remote sensor RF tag has priority. The choice does not entail a big difference in the communication capacity.

CP scheme not only leads to sub-optimized performance, but also minimizes implementation complexity (execution time). Since achieving better optimality normally requires more complicated resource allocation algorithms, sub-optimal algorithms with lower complexity are of practical interests. The time complexity of CP is $O(N^2)$ which makes it more practical and better compared to the other schemes. Figure 11 shows the comparison of simulation time calculated theoretically for brute force method and CP scheme. It can be seen that the execution time for CP scheme is far less than the brute force method.

In Appendix B, we additionally report the performance of CP when the assumptions in the channel allocation are modified in two ways. Firstly, we introduce service grade to prioritize the channel allocation. We show that high service grade sensors could be allocated to good quality channels simply by introducing a service grade coefficient in CP. Secondly, we examine the case where the number of available channels are larger than the total sum of the sensors bandwidth. We show that the spare frequency channels can be effectively used to increase the total performance.

5. Conclusion

The challenge of subcarrier allocation in variable bandwidth MSMA is the arbitration among bandwidth and the distance of sensor RF tag. The general rule of thumb is to allocate one third of available bandwidth to remote or wide bandwidth sensor RF tags since the low frequencies entail more interference in the available bandwidth than the high frequencies. To prioritize either a wide bandwidth and remote sensor RF tag or a narrow bandwidth and close sensor RF tag, we introduce total contamination power index with which we can handle the two criteria simultaneously. By using the total contamination index, the original permutation combinatorial problem $O(N!)$ can be simplified to $O(N^2)$ problem, thus significantly reducing the computation time. Yet the proposed method achieves almost equivalent performance in terms of communication capacity and fairness compared with the true optimized solution.

Acknowledgments

This work is supported by Ministry of Internal Affair and Communications Japan under SCOPE 155003007.

References

[1] B. Ando, S. Baglio, and C. Trigona, "Autonomous sensors: From standard to advanced solutions [Instrumentation notes]," IEEE Instrum. Meas. Mag., vol.13, no.3, pp.33–37, 2010.
[2] Y. Kawakita and H. Ichikawa, "Ubiquitous sensing platform for energy harvesting wireless sensor," J. Society of Instrument and Control Engineers, vol.52, no.11, pp.966–972, 2013 (in Japanese).
[3] Z. Wang, F. Bouwens, R. Vullers, F. Petré, and S. Devos, "Energy-autonomous wireless vibration sensor for condition-based maintenance of machinery," SENSORS, 2011 IEEE, pp.790–793, 2011.
[4] W.C. Wilson and G.M. Atkinson, "Passive wireless sensor applications for NASA's extreme aeronautical environments," IEEE Sensors J., vol.14, no.11, pp.3745–3753, 2014.
[5] Analog Devices, MEMS wireless vibration sensing enables remote monitoring of industrial machine health, Analog device news release, June 4, 2013.
[6] S.E. George, M. Bocko, and G.W. Nickerson, "Evaluation of a vibration-powered, wireless temperature sensor for health monitoring," Aerospace Conference, 2005 IEEE, pp.3775–3781, IEEE, March 2005.
[7] S. Adee, "Wireless sensors that live forever," IEEE Spectr., vol.47, no.2, p.14, 2010.
[8] M.R. Akhondi, A. Talevski, and T.H. Chou, "Prototype design and analysis of wireless vibration sensor," Broadband, Wireless Computing, Communication and Applications (BWCCA), 2010 International Conference on, pp.818–823, IEEE, Nov. 2010.
[9] Y. Igarashi, Y. Sato, Y. Kawakita, J. Mitsugi, and H. Ichikawa, "A feasibility study on simultaneous data collection from multiple sensor RF tags with multiple subcarriers," RFID (IEEE RFID), 2014 IEEE International Conference on, pp.141–146, IEEE, April 2014.
[10] Y. Igarashi, N. Rajoria, J. Mitsugi, Y. Kawakita, and H. Ichikawa, "A performance analysis of interference rejection technique in multi-subcarrier multiple access," RFID Technology and Applications (RFID-TA), 2015 IEEE International Conference on, pp.33–38, IEEE, Sept. 2015.
[11] N. Rajoria, Y. Igarashi, J. Mitsugi, Y. Kawakita, and H. Ichikawa, "Comparative analysis on channel allocation schemes in multiple subcarrier passive communication system," IEICE Trans. Commun., vol.E98-B, no.9, pp.1777–1784, Sept. 2015.
[12] R. Jain, D.M. Chiu, and W.R. Hawe, A Quantitative Measure of Fairness and Discrimination for Resource Allocation in Shared Computer System, vol.38, Eastern Research Laboratory, Digital Equipment Corporation, Hudson, MA, 1984.
[13] Z. Hou, D. Wu, and Y. Cai, "Subcarrier and power allocation in uplink multi-cell OFDMA systems based on game theory," Communication Technology (ICCT), 2010 12th IEEE International Conference on, pp.1113–1116, IEEE, Nov. 2010.
[14] T. Yan, M. Yayan, and W. Baoyun, "Energy-efficient power control and subcarrier allocation in OFDMA systems based on game theory," High Mobility Wireless Communications (HMWC), 2014 International Workshop on, pp.130–134, IEEE, Nov. 2014.
[15] http://tractool.seamcat.org/wiki/Manual/PropagationModels/ExtendedHata. [Visited: May 29, 2017]

Appendix A: MSMA Principle

The basic principle of MSMA is based on the backscatter communication system used in passive RFID. In a backscatter communication system, a reader transmits a powering continuous wave while sensor RF tags are responding. The major noise at reader is usually the phase noise of the continuous wave. The phase noise can be relaxed when we employ a subcarrier backscatter as shown in Fig. A·1.

A subcarrier can be produced by a constant rate switching of RF switch embedded in RF tag. The RF switch produces the mark/space digital responses. The time domain signal of a subcarrier whose frequency fs can be represented by an infinite repetition of the elemental signal as shown in Fig. A·2, where A_s is the amplitude of the signal. The elemental time domain subcarrier signal $s_e(t)$ can be represented by the following equations, where A_s is the amplitude of the signal.

$$s_e(t) = 0 \qquad -\frac{T_s}{2} \leq t \leq 0 \qquad (A\cdot 1)$$

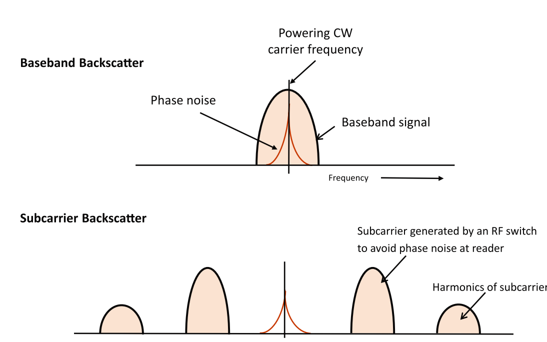

Fig. A·1 By adding a constant rate on/off keying, we can separate backscatter signal from the phase noise of powering continuous wave.

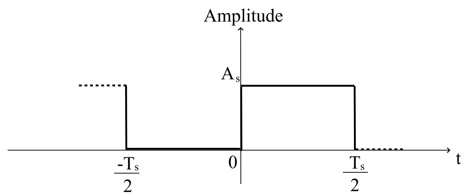

Fig. A· 2 A square wave signal considered as the subcarrier wave.

$$s_e(t) = A_s \qquad 0 \le t \le \frac{T_s}{2} \tag{A· 2}$$

The subcarrier signal in time domain shown in Fig. A· 2 can be expressed as a summation of fundamental frequency components using Fourier transform

$$s_e(t) = \frac{A_s}{2} + A_s \sum_{n=1}^{\infty} \frac{1 - \cos n\pi}{n\pi} \sin 2n\pi f_s t \tag{A· 3}$$

The summation part of the Eq. (A· 3) can be rewritten as the following

$$\begin{aligned} s_e(t) &= \frac{A_s}{2} + A_s \sum_{n=1}^{\infty} \frac{1 - \cos n\pi}{n\pi} \sin 2n\pi f_s t \\ &= \frac{A_s}{2} + \frac{2}{\pi}\left(\sin 2\pi f_s t + \frac{1}{3}\sin 6\pi f_s t + \frac{1}{5}\sin 10\pi f_s t \cdots\right) \end{aligned} \tag{A· 4}$$

From Eq. (A· 4), It can be seen that harmonic components emerge at odd multiples of primal subcarrier frequency with decaying power, where A_s and f_s denotes the amplitude of PWM signal and subcarrier frequency respectively. The harmonics conventionally prohibit the simultaneous usage of subcarriers.

MSMA features a novel interference rejection of harmonics using replicas generated from the primal subcarrier taking advantage of mathematical nature of the multiple subcarriers. Suppose four sensor RF tags backscatter at ϕ, 2ϕ, 3ϕ and 4ϕ subcarrier frequencies. The relationship between the backscatters and received signals is represented as the following matrix equation.

$$\begin{Bmatrix} R_\phi \\ R_{2\phi} \\ R_{3\phi} \\ R_{4\phi} \end{Bmatrix} = \begin{bmatrix} 1 & 0 & 0 & 0 \\ 0 & 1 & 0 & 0 \\ \frac{1}{3} & 0 & 1 & 0 \\ 0 & 0 & 0 & 1 \end{bmatrix} \begin{Bmatrix} T_\phi \\ T_{2\phi} \\ T_{3\phi} \\ T_{4\phi} \end{Bmatrix} \tag{A· 5}$$

In this equation, R_i represents the signal received at the frequency $i\phi$. T_i represents the signal transmitted concurrently from each RF tag using the subcarrier frequency $i\phi$. Note that Eq. (A· 5) is a lower triangular matrix. Thus, the transmitted signals $T_{i\phi}$ can be swiftly solved from the received signals $R_{i\phi}$ by a forward substitution. From T_ϕ to $T_{4\phi}$ can be calculated from below equations.

$$T_\phi = R_\phi \tag{A· 6}$$

$$T_{2\phi} = R_{2\phi} \tag{A· 7}$$

$$T_{3\phi} = R_{3\phi} - \frac{1}{3}R_\phi \tag{A· 8}$$

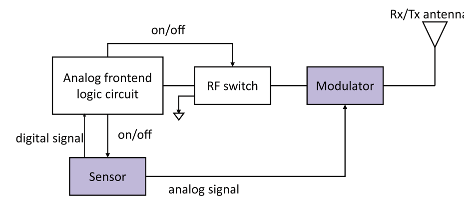

Fig. A· 3 Sensor RF tag demands minimal modification on existing RF tag.

$$T_{4\phi} = R_{4\phi} \tag{A· 9}$$

In MSMA, the sensor data can be either analog modulated with a phase modulator or digitally modulated onto the subcarrier by taking XOR of the digital data and the subcarrier toggle. A sensor RF tag in MSMA can be fabricated by only adding a sensor and a modulator (only in analog modulation case) to an identification RF tag as shown in Fig. A· 3.

Appendix B: Analysis of CP Scheme for Other Cases

B.1 When the Sensor RF Tags Have Different Service Grade (SG)

In Sect. 3, FT, NB and WB schemes have considered the distance or bandwidth parameter in the subcarrier allocation. However, the different parameter may require in the subcarrier allocation. Therefore, the proposed algorithm CP scheme redefined by introducing a factor α defines the application SG, such that the pseudo code for generalized CP scheme is modified and shown in Algorithm 6, where α is a coefficient to define SG.

Algorithm 6 Priority based CP scheme

T is a list of all sensor RF tags.
C is the total number of unit channels.
U is the used channels.
Initialize $U = 0$ and $i = 1$.
while $U <= \lceil C/3 \rceil$ **do**
  for $< j = 1 : N + 1 - i >$ **do**
    Calculate contamination power for the sensor RF tag T_j.
    multiply contamination power with α. Hence, $CP_j = CP_j * \alpha$
  end for
  Find the sensor RF tag t has minimum contamination power ($min.(CP_j)$), calculated in last step.
  Assign the sensor RF tag t to its require channels, say, c. Delete the sensor RF tag t from the list T.
  $i \to i + 1$; $U \to U + c$
end while
Arrange the list T in increasing order based on sensor RF tag location.
Pick a sensor RF tag from the list, allocate its require unit channels and continue this step.

We have considered the two different SG of sensor RF tags, lower-SG, and higher-SG. The α sets to 1 and 3 for the higher-SG and lower-SG sensor RF tags respectively, *i.e*, the lower value of α for a sensor RF tag has the higher-SG. The other simulation parameters are taken as same as in Sect. 4, whereas, the lower-SG and higher-SG sensor RF

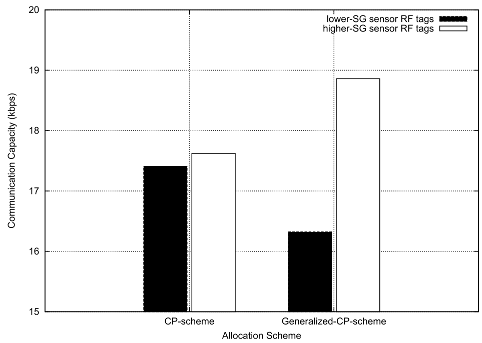

Fig. A·4 Average communication capacity with CP scheme when sensor RF tags have different SG.

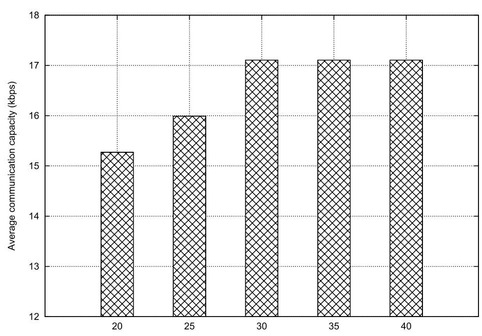

Fig. A·5 Average communication capacity with CP scheme when the number of sensor RF tags is constant and the number of available channels increases.

tags divided uniformly equal.

Figure A·4 shows the average communication capacity for CP scheme when the sensor RF tags are divided into lower-SG and higher-SG. It can be seen the CP scheme before considering the SG parameter gives an almost equal performance for both lower-SG and higher-SG sensor RF tags. However, when considering the priority factor the communication capacity for higher-SG sensor RF tags is increased because the scheme gives priority to higher-SG sensor RF tags in channel allocation.

B.2 When Available Bandwidth is More Than the Required Bandwidth

As one-third of available channels near to the central frequency generates interference to the other channels. Therefore, in the case when we have a number of channels more than the available channels we left the extra channels from near end and start allocation afterwards. By doing that the interference can be decreased among the remaining channels. Figure A·5 shows the average communication capacity for CP scheme when the number of channels is increased while a number of sensor RF tags are fixed to eight. The other simulation parameters are same as explained in Sect. 4. In simulation run, we fixed the sensor RF tags location while keeps increasing the number of available channels. It can be seen that the communication capacity increases as the number of channel increases and later it will be constant. It is because when the allocation starts after the one-third of available channels, no other channels will interfere.

Nitish Rajoria received his Master degree from Indian Institute of Technology, Hyderabad (IITH) India in Computer Science & Engineering. Currently, he is a Doctoral student in Keio University, Japan. His research interest are wireless communication, M2M communication in Internet of Things and RFID technology.

Hiromu Kamei is a Bachelor's student in Keio University. His current research interests include Wireless communication and Information Technology.

Jin Mitsugi received a B.S. from Nagoya University in 1985, M.S. and Ph.D. from Tokyo University in 1987 and 1996, respectively. He was with NTT Laboratory from 1987 pursuing research and development on satellite communication system. He has been with Auto-ID Laboratory, Japan at Keio University since 2004. His research interests are network RFID, sensor network system, satellite communications and operations research.

Yuusuke Kawakita received a B.A., an M.A. degrees and Ph.D. from Keio University in 2000, 2002 and 2008, respectively. He is an assistant professor at the University of Electro-Communications. His present research interests focus on the ubiquitous sensing and its platform architecture.

Haruhisa Ichikawa received B.S., M.S, and Dr. Eng. degrees in electrical engineering from the University of Tokyo in 1974, 1976, and 1989, respectively. He joined NTT Laboratories in 1976, where he was engaged in fundamental research on communications software and distributed computing. He created and conducted many R&D projects for software, Internet, information sharing platform, and ubiquitous networks, including business incubation. He was Executive Director of NTT Science and Core Technology Laboratory Group till 2007, and is currently Professor at the University of Electro-Communications, Tokyo.